

1 **Demographic variability and heterogeneity among individuals within and among clonal bacteria**  
2 **strains**

3 **Lionel Jouvét<sup>1,2</sup>, Alexandro Rodríguez-Rojas<sup>3</sup>, Ulrich K. Steiner<sup>1,2\*</sup>**

4  
5 <sup>1</sup> Max-Planck Odense Centre on the Biodemography of Aging, Campusvej 55, 5230 Odense, Denmark

6 <sup>2</sup> Biology Department, University of Southern Denmark, Campusvej 55, 5230 Odense, Denmark

7 <sup>3</sup> Institute of Biology, Freie Universität Berlin, Königin-Luise-Straße 1-3, 14195 Berlin, Germany

8  
9 Alexandro Rodríguez-Rojas: ORCID iD: 0000-0002-4119-8127

10

11 \*corresponding author: [usteiner@biology.sdu.dk](mailto:usteiner@biology.sdu.dk); orcid.org/0000-0002-1778-5989

12

13 This submission includes Supplementary material

14

15 **Data deposition**

16 The processed image analysis data, R code, as well as the Leslie matrices will be archived at

17 Dryad.org.

18 **Keywords:** fixed heterogeneity, dynamic heterogeneity, neutral variability, trade-off, life history

19 evolution, senescence, aging.

20

## 21 **Abstract**

22 Identifying what drives individual heterogeneity has been of long interest to ecologists, evolutionary  
23 biologists and biodemographers, because only such identification provides deeper understanding of  
24 ecological and evolutionary population dynamics. In natural populations one is challenged to  
25 accurately decompose the drivers of heterogeneity among individuals as genetically fixed or selectively  
26 neutral. Rather than working on wild populations we present here data from a simple bacterial system  
27 in the lab, *Escherichia coli*. Our system, based on cutting-edge microfluidic techniques, provides high  
28 control over the genotype and the environment. It therefore allows to unambiguously decompose and  
29 quantify fixed genetic variability and dynamic stochastic variability among individuals. We show that  
30 within clonal individual variability (dynamic heterogeneity) in lifespan and lifetime reproduction is  
31 dominating at about 82-88%, over the 12-18% genetically (adaptive fixed) driven differences. The  
32 genetic differences among the clonal strains still lead to substantial variability in population growth  
33 rates (fitness), but, as well understood based on foundational work in population genetics, the within  
34 strain neutral variability slows adaptive change, by enhancing genetic drift, and lowering overall  
35 population growth. We also revealed a surprising diversity in senescence patterns among the clonal  
36 strains, which indicates diverse underlying cell-intrinsic processes that shape these demographic  
37 patterns. Such diversity is surprising since all cells belong to the same bacteria species, *E. coli*, and still  
38 exhibit patterns such as classical senescence, non-senescence, or negative senescence. We end by  
39 discussing whether similar levels of non-genetic variability might be detected in other systems and  
40 close by stating the open questions how such heterogeneity is maintained, how it has evolved, and  
41 whether it is adaptive.

42 Heterogeneity among individuals has important ecological and evolutionary implications because it  
43 determines the pace of ecological and evolutionary adaptation and shapes eco-evolutionary feedbacks  
44 (Hartl and Clark 2007, Steiner and Tuljapurkar 2012, Vindenes and Langangen 2015). Despite  
45 substantial methodological and empirical efforts, it remains challenging to unambiguously differentiate  
46 the causes that drive the observed heterogeneity among individuals in their life courses, their traits, and  
47 their fitness components (Steiner and Tuljapurkar 2012, Bonnet and Postma 2016, Cam et al. 2016).  
48 There is consensus that heterogeneity among individuals is caused by changes in the environment, by  
49 variation in the genotype, by the genotype-by-environment interaction, and by noise or intrinsic  
50 processes many of which show stochastic properties (Endler 1986, Finch and Kirkwood 2000,  
51 Kirkwood et al. 2005). The latter cause has either been deemed as noise associated with non-biological  
52 processes, e.g. measurement error, and with unknown hidden processes that were of little biological  
53 relevance. Alternatively, this intrinsic “noise” has been investigated for underlying biological processes  
54 with stochastic characteristics and its substantial biological implications are illustrated by quantitative  
55 genetic and population genetic studies. The interest in such intrinsic noise is best understood by its  
56 slowing of evolutionary dynamics via lowering heritabilities and enhancing genetic drift (Lande et al.  
57 2003, Hartl and Clark 2007).

58 The challenge is heightened in natural populations to decompose the observed heterogeneity into its  
59 genetic, environmental, and non-genetic, non-environmental — stochastic — component. In such  
60 populations, we are confronted with high genetic diversity and complex environmental and gene-by-  
61 environment interactions (Fitzpatrick et al. 2016). The knowledge about the genotypes at the individual  
62 level is limited (e.g. pedigree) or in many cases totally absent. Certain environmental variables are  
63 known at the population level, but micro-environmental differences are less explored. The response of

64 individuals to the known population level environmental factors varies — e.g. due to gene-by-  
65 environment interactions — and individuals are differently affected by the population level  
66 environment, e.g. not all individuals are exposed equally. Ecologists agree on that one cannot  
67 encompass the whole complexity of natural systems and hence the additional variance is a combination  
68 of error and some hidden drivers of heterogeneity. The aim remains identifying the cause of this  
69 additional heterogeneity since only such identification allows forecasting of and understanding of  
70 evolutionary and ecological population dynamic processes (Lande et al. 2003, Tuljapurkar et al. 2009,  
71 Steiner et al. 2010).

72 Not only empirical challenges occur when trying to decompose the observed variance in natural  
73 populations, from a methodological point of view challenges await us. Various statistical approaches  
74 aim at classifying the hidden heterogeneity as either fixed at birth, e.g. additive genetic effects or  
75 maternal effects, or as dynamic heterogeneity, heterogeneity generated during the course of life  
76 (Tuljapurkar et al. 2009, Steiner et al. 2010, Steiner and Tuljapurkar 2012, Bonnet and Postma 2016,  
77 Cam et al. 2016, Hartemink et al. 2017). Such models, be they based on mixed effect models, Markov  
78 chains, hidden Markov chains, covariate models or related models, are biased and cannot reveal the  
79 accurate underlying mechanism unless the contributing factors and the underlying error structure is  
80 known (Bonnet and Postma 2016, Cam et al. 2016). This applies to both so-called neutral models that  
81 base their arguments on dynamic heterogeneity — heterogeneity best described by stochastic  
82 transitions among stages that shape individual life courses —, and adaptive selective models that base  
83 their arguments on fixed heterogeneity, variability among individuals fixed at birth described by  
84 genetic differences or maternal effects. Note, in the fixed type of models there remains a large

85 unexplained residual error, a variance of unknown origin, and even models that combine dynamic and  
86 fixed heterogeneity suffer from biased estimations.

87 To circumvent these empirical and methodological challenges faced in natural populations, we used  
88 here cutting-edge microfluidic technologies on a simple bacterial system in the lab, *Escherichia coli*.  
89 This system, in combination with age-structured matrix population models, allowed us to  
90 unambiguously decompose and quantify fixed, genetic variability and dynamic, stochastic variability  
91 among individuals. The highly-controlled environment of the microfluidic system excluded extrinsic  
92 environmental variation and gene-by-environment variation, sharpening the focus on decomposing  
93 genetic and non-genetic and non-environmental individual variability. We defined all genetic  
94 variability as the variance among seven (clonal) bacteria strains in their mean fitness components. We  
95 call this among strain genetic variability in fitness components fixed heterogeneity. This fixed  
96 heterogeneity is set in relation to dynamic heterogeneity, the variability in fitness components among  
97 individuals within strains. This dynamic heterogeneity is generated by cell intrinsic processes and can  
98 be best described as neutral individual heterogeneity. At least it is non-genetic and non-environmental  
99 induced variability, and demographic characteristics are not heritable between mother and daughter  
100 cells (Steiner and Tuljapurkar 2012, Steiner et al. 2017). As expected, fixed, among strain genetic  
101 variability was modest compared to the substantial within strain variability in reproduction and  
102 survival. Variance in lifespan within strains explained ~88% and 12% was related to among strain  
103 variance in lifespan. Variance in lifetime reproductive success within strains explained ~82% and 18%  
104 was related to among strain variance. Our finding does not imply that the genetic variability is not  
105 relevant, it just highlights that there is large amount of heterogeneity expressed within strains that is  
106 neither genetically nor environmentally driven and can therefore be described as neutral.

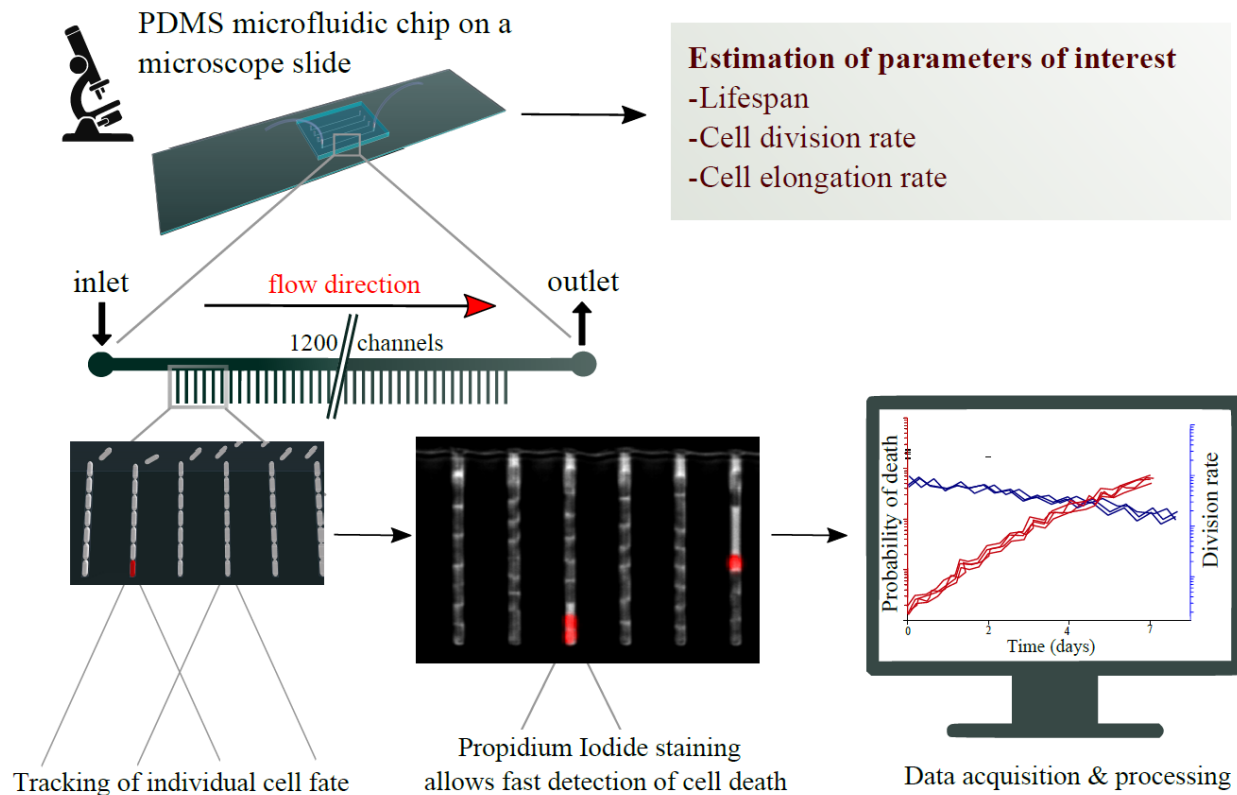
## 107 **Material and methods**

108 The study organism we worked with is *E. coli*, a rod-shaped bacteria and molecularly well explored  
109 model organism. We defined each bacteria cell as an individual. Individuals grow (elongate) and  
110 reproduce by binary fission, a division in two usually equal sized cells. Note that these cells are  
111 functionally unequal, and such functional asymmetry is crucial otherwise a mother cell would divide  
112 into two identical daughter cells and thereby the original mother cell would “die” (Johnson and Mangel  
113 2006, Tyedmers et al. 2010). In addition, populations with perfect symmetric dividing cells are not  
114 viable over multiple generations if oxidative damage accumulates in cells as described for many aging  
115 processes including those for bacteria (Ackermann et al. 2007, Evans and Steinsaltz 2007, Lindner and  
116 Demarez 2009, Tyedmers et al. 2010). The asymmetry in division allows to distinguish a mother cell,  
117 the cell that holds the old pole of the cell wall, and a daughter cell, the offspring cell that inherits the  
118 more recent pole of the cell wall (Stewart et al. 2005). Even though senescence patterns are observed  
119 and individual cells age, the change in mortality rates across age is not determined by the age of the cell  
120 pole itself even though it is correlated (Steiner et al. 2017). It is not the cell pole age, but the cytoplasm  
121 content that influences mortality rates. While the mother cells senesce, the daughter cells are thought to  
122 be rejuvenated (Ackermann et al. 2007), but this rejuvenation seems only to be perfect for daughters of  
123 young mothers and not for daughters of old mothers (Steiner et al. 2017). Further, among isogenic  
124 bacteria the lifespan of the mother does not correlate with the lifespan of the daughter, which suggests  
125 that the asymmetry at fission has a dominating stochastic component to it (Steiner et al. 2017). Despite  
126 intensive mechanistic research on the factors involved in the functional asymmetry, none of the factors  
127 have been identified as the actual cause or consequence of the functional difference that determine the  
128 cell fates (Nyström et al. 2007, Lindner and Demarez 2009, Tyedmers et al. 2010). The more

129 quantitative demographic approach we have taken here does not focus on the within cell mechanistic  
130 factors but rather aims at decomposing the genetic and dynamics components driving individual  
131 heterogeneity.

132 For our experiments we used a bacterial microfluidic system called mother machine (Wang et al. 2010,  
133 Steiner et al. 2017) (Fig.1). This system allows tracking thousands of individual cells via time-lapse  
134 phase-contrast microscopic imaging. Using these time-lapse images, we determined for each (mother)  
135 cell the lifespan, the timing and number of divisions, as well as the size and cell elongation throughout  
136 their lives. We identified cell death by propidium iodide, a chemical that enters the cell after the cell  
137 wall lysed and emits a strong red fluorescent signal when it binds to the DNA. We only collected and  
138 tracked data on the (old pole) mother cell, the bottom most cell of the dead-end side channels (Fig. 1);  
139 daughter cells are pushed out into the main, laminar flow channel and washed away and cannot be  
140 tracked throughout their lives.

## Experimental setup to assess individual heterogeneity in *E. coli*



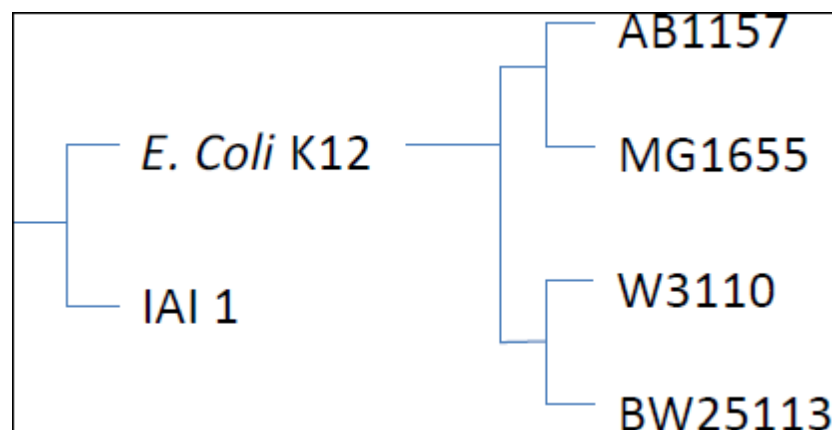
141

142 Fig. 1: Experimental setup of microfluidic system to track individual bacteria cells throughout their  
143 lifetime. The main (horizontal) channel with the constant laminar flow connects directly the inlet and  
144 outlet and provides the cells, that grow in the vertical side channels, with fresh media. The vertical  
145 smaller side channels hold at their dead end the focal (mother) cell, which is the bottom most cell in  
146 each side channel.

147 To control the genetic variability, we conducted separate experiments for seven different isogenic  
148 strains. Based on the individual demographic data of the tracked cells, we estimated hourly age-specific  
149 survival and reproduction rates which we used to parameterize age-specific matrix models (Leslie  
150 matrices), one model for each of the seven isogenic strains. We selected the seven *E. coli* strains based



151 on their common use as model organisms in the lab (K12 variants) and complemented them by a  
152 genetically distinct strain (Fig. 2). Details on the experiments, microfluidic chip production and strains  
153 are given in the online Supplementary material.



154  
155 Fig. 2: Phylogenetic relationship among the different *E. coli* strains.

156

#### 157 Data analysis

158 To analyse our individual level demographic data (each mother cell is an individual) that was collected  
159 by time-lapse imaging, we parameterised discrete age-structured population models formulated as  
160 Leslie matrices. The time-lapse images were taken at 4-minute intervals, and therefore we recorded for  
161 each focal (mother) cell whether it had divided, how much it had grown, and whether it died within a 4-  
162 minute time interval. For each isogenic strain, we formulated one Leslie matrix,  $A$  (Table 1). Since not  
163 all cells were dead at the end of the experiments we right censored these cells. To parameterise the age-  
164 structured Leslie matrix models we calculated hourly division and survival rates rather than 4-minute  
165 rates as collected via the time-lapse imaging. Hourly rates were calculated to reduce uncertainty due to

166 sampling variability of small sample sizes and to increase the accuracy of calculating vital rates. To be  
167 precise, for each strain, we calculated the age-specific survival probabilities from time  $t$  to time  $t+1$   
168 (one hour time steps) by the fraction of cells alive at time  $t+1$  over those cells alive at time  $t$ . For  
169 reproduction rates, we calculated the average number of divisions a cell underwent between time  $t$  and  
170 time  $t+1$  given that the cell was alive, this was done for each strain separately. The survival  
171 probabilities entered the sub-diagonal parameters of the strain specific Leslie matrix, and the age-  
172 specific division rates entered the top row of the strain specific Leslie matrix.

173 We choose a Leslie matrix model approach since these models conveniently and directly link  
174 individual level data, as collected by our experiments, to population level properties, including the  
175 population growth rate and the generation time. The direct calculation of vital rates, as commonly done  
176 for matrix models, rather than fitting function parameters as for instance done in logistic regressions,  
177 provided great variability and accuracy in estimating the demographic parameters. The close match  
178 between observed data and the matrix elements can be seen in Fig. A4. Such direct parameter  
179 calculation usually ignores the effect of sampling variability, and effects of sampling variability can be  
180 substantial for small populations (<100 individuals) with low survival (<0.5) (Fiske et al. 2008). In our  
181 study both survival rates and sample sizes (312 to 1017 cells per strain) were well above levels were  
182 substantial influences of sample variation is expected (Fiske et al. 2008). If such sampling variability  
183 would significantly influence our results, we would also expect to see low replicability among  
184 subsamples within strains, a pattern not found in our study (Fig. A3).

185 We assumed that all individual cells that were initially loaded into the microfluidic device are  
186 of age 0. We know that this assumption is partly violated. Based on stable-age theories of exponentially  
187 growing populations the age distribution is highly right skewed (Fig. A2), and less than 30% of the  
188 loaded cells are older than 1h, i.e. >70% of the individuals are of age<1h (Steiner et al. 2017).

189 Unfortunately, we have no means to determine which of the initially loaded cells are older than 1h.  
190 Convergence to a stable-age distribution, as assumed by matrix population models, should be fast in  
191 populations with vital rates as we computed for our bacteria populations. Further, such stable-age  
192 distribution should be closely achieved in the exponentially growing populations under constant and  
193 non-limiting growth conditions, as the ones the initially loaded mother cells are originating from. For  
194 the above reasons, potential transient dynamics are not expected to have large influences (SI Fig. A2)  
195 (Steiner et al. 2017).

196 We used the seven strain specific Leslie models,  $A$ , to compute for each strain the following  
197 demographic parameters: the population growth rate,  $\lambda$ , the cohort generation time,  $T_c$ , the mean and  
198 among individual variance in lifespan, the mean and among individual variance in lifetime  
199 reproduction, the stable age distributions, and the age-specific reproductive values. Equations for  
200 estimating the demographic parameters are listed in Table 1, for proofs and further details please see  
201 Caswell (2001), Steiner and Tuljapurkar (2012), and Steiner et al. (2014) . The computed demographic  
202 parameters are shown in Table 2, Fig. A1 and Fig. A2. We choose to estimate the mean and variance in  
203 fitness components — lifespan and reproduction — based on the Leslie matrix rather than on the  
204 original data to minimize the influence of different levels of right censoring. Fig. 3 shows the original  
205 observed data with the right censoring, and Fig. A4 shows the close match between the age at death  
206 distributions based on the original observed data and the age at death distribution predicted by the  
207 Leslie model.

208 We decomposed the among strain variance (fixed genetic) and within strain (dynamic) variance  
209 in fitness components using the seven strain specific estimates of the variance in lifespan,  $VarL_i$   
210 (equations: Table 1, values: Table 2; subscript  $i$  indicates the strain) and estimated the mean of these

211 seven strain specific values. This mean variance ( $\overline{VarL}$ ) provided us with the mean within strain  
212 variance in lifespan. We followed the same procedure to compute the mean within strain variance in  
213 reproduction ( $\overline{VarexR}$ ). We related these mean (within strain) variances ( $\overline{VarL}$  and  $\overline{VarexR}$ ) to the  
214 variance in the strain means ( $Var(exL_i) = ex[(exL_i - \overline{exL})^2]$ ;  $Var(exR_i) = ex[(exR_i - \overline{exR})^2]$ )  
215 respectively. We equally weighted each strain estimate, i.e. we did not consider that some strains had  
216 more cells the estimates are based on compared to others. Our results are qualitatively robust to this  
217 assumption.

218

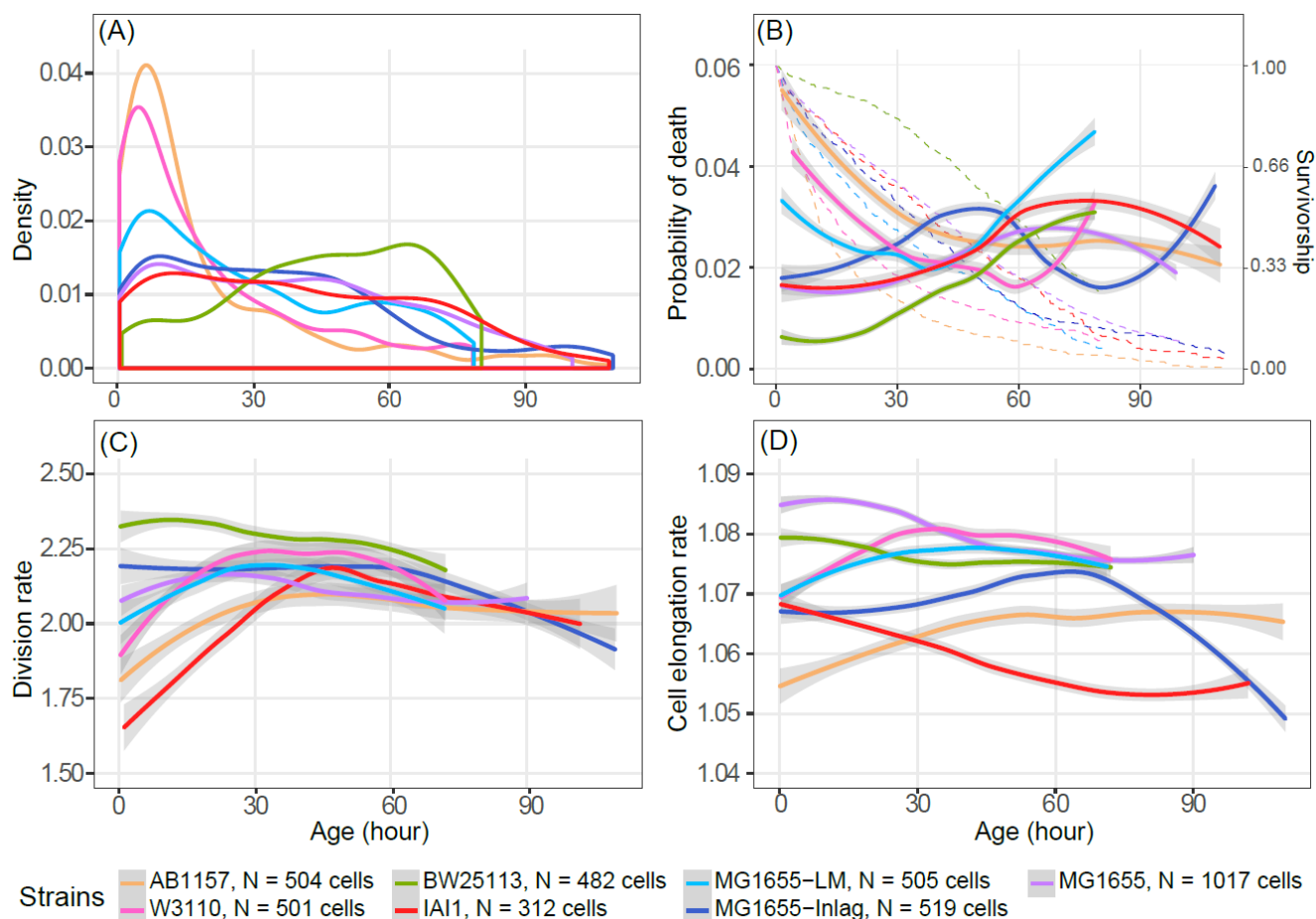
## 219 **Results**

220 Our results are based on a total of 3840 individual cells (3461 were tracked over their whole lifespan  
221 and 379 were right censored) (Fig. 3A, B). The cells in our experiments originated from seven isogenic  
222 strains (312 to 1017 cells per strain; mean  $549 \pm 202$  SD) (Table 2). Population growth rates,  $\lambda$ , varied  
223 between 1.74 and 2.25 per hour (mean  $2.06 \pm 0.17$  SD), mean lifetime reproductive success (net  
224 reproductive rate,  $R_0$ ) varied, between 42 and 128 individuals (mean  $75 \pm 27$ ), generation time,  $T$ ,  
225 varied between 2.3 and 3.29 hours (mean  $2.57 \pm 0.34$  SD), and cohort generation time,  $T_C$ , varied  
226 between 31 and 77 hours (mean  $52.9 \pm 16.7$  SD) (Table 2). The coefficient of variation in lifespan  
227 within strains ( $CV = \text{within strain SD in lifespan} / \text{mean strain lifespan}$ ) varied between 0.4 and 1.2 (mean  
228  $0.8 \pm 0.2$ ), and was highly correlated to the CV of lifetime reproductive success within strains (0.4 to  
229 1.3; across strain mean  $0.8 \pm 0.3$ ). Mean within strain variance in lifespan was high at  $766 \text{ h}^2$  compared  
230 to variance in mean lifespan among strains at  $105 \text{ h}^2$ . Similarly, mean within strain variance in lifetime  
231 reproductive success was high at  $3230 \text{ ind}^2$  compared to variance in mean lifetime reproductive success  
232 among strains at  $708 \text{ ind}^2$ . Based on the variances within and among strains, ~88% of the variance in

233 lifespan comes from within strains and 12% of variance in lifespan is caused by among strain variance.  
234 For lifetime reproductive success within strain variance dominates in generating ~82% of variance and  
235 18% was observed among strains.

236 We illustrate the high variability in lifespan among individuals within strains in Fig. 3A. The  
237 corresponding age specific mortality patterns (Fig.3B) highlight the diversity in demographic patterns  
238 among strains. Such diversity is remarkable considering that all strains belong to the same species, *E.*  
239 *coli*, and have experienced identical constant environments throughout the experiments (highly  
240 controlled medium, nutrition, and temperature). Some strains showed negative chronological  
241 senescence with declining mortality with increasing age (AB1157), others showed more bathtub shapes  
242 with declining mortality early in life followed by classical senescence later in life (MG1655\_LM,  
243 W3110), still others showed only classical senescence with increasing mortality with age (BW25113),  
244 or finally others first showed increased mortality early in life before exhibiting declining mortality later  
245 in life (MG1655, IAI1). Some of the late age mortality rates were estimated on small numbers of cells,  
246 and the very old age patterns (e.g. MG1655-Inlag showing steep rising mortality above 90h) should not  
247 be over-interpreted due to uncertainty from sampling variability. We also revealed substantial among  
248 strain diversity in age specific division rates (Fig. 3C) and cell elongation rates (cell growth rates) (Fig.  
249 3D). Most strains reached somewhat similar division rates after age 45h and showed moderate  
250 decreases in division (reproductive senescence) at older ages. At younger ages division rates differed  
251 substantially among the different strains, by either being fairly constant or increasing with age. Cell  
252 elongation rates (cell growth rates) showed similar diverse patterns among strains as mortality. Cell  
253 elongation (cell growth) increased (e.g. AB1157), decreased (e.g. IAI1), or first increased and then  
254 decreased (e.g. MG1655-Inlag) with increasing age. The age-specific reproductive values and stable

255 stage distributions for the seven different strains are shown in the Appendix (Supplementary material  
 256 Appendix 1, Fig. A1, A2).



257

258 Fig. 3: Lifespan distribution (A), probability of death (B), division rate (C), and cell elongation rate (D) of seven  
 259 different bacteria strains plotted against age in hours. For (B) also survivorship curves are plotted as dashed  
 260 lines. 95 % CI are shown in grey shading (B, C, D). For B and C hourly rates are shown, for D rates per 4min  
 261 intervals are shown. Note, cells of the different strains are truncated (right censored) at different ages. All rates  
 262 have been loess (program R) smoothed.

263 **Discussion**

264 We showed that fixed heterogeneity in lifespan and reproduction, i.e. the genetic contribution, is  
265 moderate compared to the heterogeneity among individuals within strains, the neutral dynamic, and  
266 non-genetic and non-environmental, heterogeneity. Only our highly-controlled study system allows  
267 such an accurate and direct decomposition of heterogeneity in genetic and non-genetic contributions.  
268 Under less controlled setting, as in natural populations, we could not decompose the causes of mortality  
269 and reproduction without bias (Steiner and Tuljapurkar 2012, Bonnet and Postma 2016, Cam et al.  
270 2016). Despite the dominating variability within strains, we detected significant and evolutionary  
271 important variability among strains. This selective difference is best illustrated by the differences in  
272 population growth rate,  $\lambda$ , which would lead to fast changes in genotype frequencies. The differences in  
273  $\lambda$  directly inform us on each of the strains fitness, i.e. how fast the different strains would grow and  
274 compete against each other under the exponential growth conditions in our experiments. In our system,  
275 environmental conditions exclude any density dependence, reduce extrinsic environmental variability  
276 to a level that is negligible, and provide non-limiting conditions that promote exponential population  
277 growth as assumed under stable stage theories.

278 The within strain heterogeneity is partly illustrated by the coefficient of variation of the fitness  
279 components. The estimates we found here are comparable to less controlled systems and more complex  
280 organisms. In laboratory systems of other isogenic individuals under lab conditions the coefficient of  
281 variation (CV) ranges between 0.24 to 1.33 in lifespan [*Caenorhabditis elegans* 0.24-0.34 (Finch and  
282 Kirkwood 2000, Kirkwood et al. 2005), *Caenorhabditis briggsae* 0.31-0.51 (Schiemer 1982),  
283 *Saccharomyces cerevisiae* (0.37)(Kennedy 1994)]. Less genetically controlled lab populations do not  
284 differ much from these patterns in the CV of lifespan: laboratory reared mice (0.19-0.71)(Finch and  
285 Kirkwood 2000), *Drosophila melanogaster* 5.98-13.48 (Curtsinger et al. 1992). Even under less  
286 controlled conditions in the field, for instance, a plant species, *Plantago lanceolatum*, shows a CV 0.96

287 for lifespan, and 3.97 for reproduction (Steiner et al. unpublished) and such estimates seem not  
288 exceptional even in populations where we do not know the genetic or the environmental contributions  
289 (Tuljapurkar et al. 2009, Steiner et al. 2010). Even though in less controlled systems this CV includes  
290 contributions of fixed and dynamic heterogeneity, the comparatively similar estimates between highly  
291 controlled lab systems and natural systems might indicate that neutral variability could be substantial  
292 not only in controlled lab populations. If one sees it the other way around, our somewhat highly  
293 artificial and very simple model system shows surprisingly little difference in CV of fitness  
294 components compared to more natural systems.

295 The ambiguity of estimates in natural populations about fixed and dynamic heterogeneity generating  
296 observed variances has resulted in a heated debate about neutral and adaptive contributions to this  
297 heterogeneity (Bonnet and Postma 2016, Cam et al. 2016). As with other neutral theories in molecular  
298 biology (Leigh 2007), or community ecology (Hubbell 2001), the neutral theory of life histories  
299 (Steiner and Tuljapurkar 2012) has been attacked based on a common misunderstanding behind neutral  
300 theories, that is, the erroneous claim that all variability is neutral. We know that all neutral theories are  
301 wrong (Leigh 2007). Any natural population includes selective differences, but the neutral theory  
302 illustrates to what extend variability might be neutral (in its theoretical extreme). To date, we do not  
303 have the means to unambiguously differentiate the causes driving the observed heterogeneity in natural  
304 populations. In our study, we show how substantial neutral heterogeneity can be in a simple bacterial  
305 system. This large heterogeneity might be surprising since the strains are highly adapted to the lab  
306 conditions. Selection has not managed to get rid of this variability, and the question arises how such  
307 neutral variability is maintained and if it is adaptive.



308 Labeling heterogeneity among individuals as neutral is often perceived with skepticism, since apparent  
309 random processes might have a deterministic hidden biological cause. From a deterministic point of  
310 view, each individual would be born with an intrinsic clock that determines its life course. Such a clock  
311 would have no genetic or epigenetic component, because mother and daughters life course are not  
312 correlated (Steiner et al. 2017). We believe the bacteria system can partly inform on distinguishing  
313 among such a deterministic viewpoint and an understanding that explains these hidden underlying  
314 processes to be generated by random events showing, e.g. showing stochastic characteristics.

315 Numerous molecular and biochemical processes that are assumed to shape life courses of individuals  
316 have been identified for *E. coli*, many of them related to direct or indirect oxidative processes, but as in  
317 any other system the molecular and biochemical process of aging for *E. coli* is not fully understood  
318 (Kirkwood et al. 2005, Raj and van Oudenaarden 2008, Lindner and Demarez 2009, Gómez 2010).  
319 Many of these mechanisms show in themselves stochastic properties, including e.g. stochastic gene  
320 expression, protein folding and misfolding, and their potential cascading effects up to the organism  
321 level (Elowitz et al. 2002, Lindner and Demarez 2009, Balázsi et al. 2011, Ackermann 2015). Despite  
322 these detailed insights on biochemical and molecular mechanisms that regulate intrinsic cellular  
323 processes, linking them to the individual life course remains challenging (Lindner et al. 2008, López-  
324 Otín et al. 2013). Such difficulties are expected if stochastic properties within the cells characterize  
325 these processes.

326 Our approach using Leslie models, only takes the age of the cell into account and averages individuals  
327 within the strains across traits, be they morphological (e.g. cell size), (stochastic) gene expression, or  
328 asymmetry in protein aggregates. Such averaging across trait variability should reduce the calculated  
329 variances in lifespan and reproduction among individuals belonging to the same strain, since stage

330 dispersion in reproduction (among ages) caused by trait variability is reduced (Steiner et al. 2014). We  
331 could have included traits such as cell size, by extending our models to age-stage structured matrix  
332 models, formulated either as classical Lefkovitch matrixes or integral projection versions of matrix  
333 models (Caswell 2001, Ellner and Rees 2006). However, increasing the parameter space trades off  
334 against accuracy of parameter estimates due to sampling variability. Also, cell elongation and division  
335 rates are correlated in *E. coli* and therefore the Leslie matrices include — in the age dispersion in  
336 reproduction — part of the variability in cell size (Steiner et al. 2017). We aimed at a simple  
337 demographic model (Leslie matrix) that provides realistic and accurate estimates (Fig. A4). Extending  
338 these simple model to more complex models should be done in future studies. Among strain variance in  
339 fitness components should not be substantially influenced by averaging across individual trait  
340 variability. Obviously, we might have missed to explore important traits that are predominantly  
341 affected by the genetic differences among the strains. However, under our experimental conditions  
342 such traits, even if they had been highly differentiated among strains, did not have a significant  
343 influence either on reproduction or survival and therefore did not increase variability among strain  
344 fitness ( $\lambda$ ). Using Leslie models directly linked the individual level data to population level properties  
345 without additional fitting of model parameters (Fig. A4). Fitting accurate functions to the somewhat  
346 complex demographic age patterns (Fig. 3) would have been challenging with other models. The Leslie  
347 matrix approach we choose provides accurate description at the population level, even though at older  
348 ages parameter calculation suffer from sampling variability. Such uncertainty at old ages should not  
349 strongly influence the overall variance decomposition, since the few individuals that live to old ages do  
350 not weigh heavily on the overall variance estimation.

351 We choose experimental conditions that reduced variance in certain traits, e.g. cell size. For instance  
352 we choose minimum medium M9 that reduces variance in division size (and size after division)  
353 compared to complex medium (Gangan and Athale 2017). Minimum medium M9 also decreases the  
354 rate of filamentation — a stress response where the cell continues to elongate without dividing. Under  
355 M9 conditions, filamentous cells rather died than recovering from filamenting by dividing into normal  
356 sized cells. Such recovery is frequently observed under complex media (Wang et al. 2010). Differences  
357 in experimental setup (e.g. starting with exponential or stationary growth cells, type of medium, strains  
358 explored, culturing devices used) make it challenging to direct compare to other single cell or batch  
359 culture *E. coli* studies, and even estimates within batch culture studies on growth rates are highly  
360 variable (Helmstetter 1968, Dennis and Bremer 2008). Compared to batch cultures grown on the same  
361 M9 media, our estimated exponential growth rates,  $\lambda$ , are high, though such increase in growth rates are  
362 expected and known for comparisons between single cell estimates and batch culture estimates that are  
363 in any case difficult to directly compare (Reshes et al. 2008) (Fig. A4).

364 In interpreting our results, we must be aware that all strains are subjected to some level of right  
365 censoring (mean: 1.4% to 26.3%; SD  $9.3\% \pm 8.8$ ). The number of individuals suffering from this  
366 censoring differs among the different strains and might therefore bias our results differently. We aimed  
367 at reducing the effect of the right censoring by estimating demographic parameters from Leslie  
368 matrices with open age brackets for the last age class (Fig. A4).

369 Another criticism on our data is that experiments are not entirely independently replicated. Each  
370 mother cell sits in its own little side channel, but the cells of each strain are still confounded in being  
371 loaded in the same microfluidic chip and have been provisioned by the same highly controlled laminar  
372 flow. The amount of nutrients delivered to the cells is magnitudes larger compared to the amount all

373 cells could consume; hence there should be no limitation of resources or any difference in access to  
374 resources among cells. Preliminary experiments (Jouvet & Steiner unpublished) also indicate that  
375 diffusion properties among the individual side channels are very similar, ascertaining that extrinsic  
376 environmental variation the individual cell experience in the microfluidic device are negligible. Despite  
377 the confounding effects, we are convinced that our data is representative since patterns among  
378 independent flow channels are highly replicable as we illustrate in the SM for one of our strains  
379 (Supplementary material Appendix 1, Fig. A3). Further if individual side channels would differ in their  
380 environments we would expect a correlation between mother and daughter cells in their lifespan, but  
381 such correlation has not been found in other studies (Steiner et al. 2017).

382 Our results also illustrate how genetic variability, even within a species, can shape very diverse  
383 senescence patterns, both in survival and reproduction. Phylogenetically more closely related strains  
384 (Fig. 2) do not necessarily show more similar demographic patterns compared to less closely related  
385 strains (e.g. AB1157, MG1655, W3110). This raises interesting questions for comparative demography  
386 where a single population of a species is frequently assumed to be representative for each species  
387 (Jones et al. 2014). Even under our highly controlled environmental condition we see great diversity in  
388 demographic patterns and it would be interesting to compare multiple natural populations of the same  
389 species to investigate how persistent demographic patterns within species are in nature.

390

391 Given the highly controlled environment and the high genetic control our system also open doors to  
392 investigate basic evolutionary theories of life history (Hamilton 1966, Stearns 1992). Such theories  
393 base much of their arguments on a fundamental tradeoff between reproduction and survival or early  
394 versus late life trade-offs. One of the challenges of assessing such trade-offs include that individuals,

395 populations, or genotypes receive different amounts of resources (energy or nutrients) and these  
396 differences might override the underlying trade-offs (van Noordwijk and de Jong 1986). Our highly  
397 controlled environment and the clear distinction of genotypes therefore provide a nice opportunity to  
398 reveal such tradeoffs that are hard to reveal in natural populations (Metcalf 2016). Based on the  
399 theories, we predict that strains with high mortality should exhibit high reproduction (high division and  
400 cell growth rates). Such simple expectations are not met, strains with relatively low mortality (e.g.  
401 BW25113) also showed high cell elongation and division rates, while other strains showed somewhat  
402 opposite patterns (e.g. AB1157). Similarly we did not detect clear age-specific trade-offs between early  
403 and late survival or early and late reproduction and their interaction as predicted by evolutionary  
404 theories of aging (Medawar 1952, Williams 1957, Hamilton 1966). Strain IAI1 for instance showed  
405 senescence in survival and in cell elongation rates, but increased in reproduction (division rate) with  
406 age, before plateauing off at old ages. Other strains (e.g. MG1655-Inlag) showed increased and  
407 decreased mortality with age and similar patterns in cell elongation, but did not show much change in  
408 division rate over much of life. Only late in life did MG1655-Inlag, reveal some reproductive  
409 senescence. We can interpret the lack of such expected relationships among survival and reproduction  
410 as a lack of genetic linkage between traits and ages, and that the underlying life-history tradeoffs are  
411 not as strong as assumed. One might argue that this system is too artificial to express such trade-offs.  
412 Still, we see familiar demographic patterns even in this simple system, and our best evidence for such  
413 trade-offs is coming from such artificial lab organisms, rather than from populations in their natural  
414 environments (Metcalf 2016). A fundamental challenge behind revealing these trade-offs is that they  
415 are expressed within individuals and not among individuals, but most of our attempts compare among  
416 individuals that belong to different groups, genotypes, populations, and species, as we do in our study.

417 Our findings unambiguously quantified fixed and dynamic heterogeneity for a simple bacterial system.  
418 We revealed that substantial variability is generated by cell-intrinsic likely stochastic processes and that  
419 the quantity and timing of these processes differ among the clonal strains, shaping diverse age-specific  
420 demographic patterns. To what extent similar levels of variability are generated by intrinsic likely  
421 stochastic processes in natural populations of simple organisms such as bacteria or more complex  
422 organisms should be explored. We discussed similarities in coefficient of variation across different  
423 level in complexity among organisms and across levels of control that suggest that our result is not  
424 exceptional. Promising attempts to overcome the unknown genetics of individuals in natural  
425 populations have been made by releasing hundreds or thousands of genetically known crossed  
426 individuals into the wild and then tracked throughout their lives (Roach 2012, Travis et al. 2014).  
427 Evidence of such experiments suggests that levels of within cross heterogeneity is substantial compared  
428 to among cross heterogeneity. How such heterogeneity is maintained, how it has evolved, and whether  
429 it is adaptive remains to be explored.

#### 430 **Acknowledgements**

431 We thank all members of the Max Planck Odense Center on the Biodemography of aging for  
432 discussions and comments. We were supported by the Max Planck Society (LJ, UKS) and SFB 973  
433 (Deutsche Forschungsgemeinschaft), project C5 (ARR).

#### 434 **References**

- 435 Ackermann, M. 2015. A functional perspective on phenotypic heterogeneity in microorganisms. - Nat.  
436 Rev. Microbiol. 13: 497–508.
- 437 Ackermann, M. et al. 2007. On the evolutionary origin of aging. - Aging Cell 6: 235–44.
- 438 Balázsi, G. et al. 2011. Cellular decision making and biological noise: from microbes to mammals. -  
439 Cell 144: 910–925.

- 440 Bonnet, T. and Postma, E. 2016. Successful by Chance? The Power of Mixed Models and Neutral  
441 Simulations for the Detection of Individual Fixed Heterogeneity in Fitness Components. - Am.  
442 Nat. 187: 60–74.
- 443 Cam, E. et al. 2016. The Conundrum of Heterogeneities in Life History Studies. - Trends Ecol. Evol.  
444 31: 872–886.
- 445 Caswell, H. 2001. Matrix population models: construction, analysis, and interpretation. - Sinauer  
446 Associates.
- 447 Curtsinger, J. et al. 1992. Demography of genotypes: failure of the limited life-span paradigm in  
448 *Drosophila melanogaster*. - Science (80-. ). 258: 461–463.
- 449 Dennis, P. P. and Bremer, H. 2008. Modulation of Chemical Composition and Other Parameters of the  
450 Cell at Different Exponential Growth Rates. - EcoSal Plus in press.
- 451 Ellner, S. P. and Rees, M. 2006. Integral projection models for species with complex demography. -  
452 Am. Nat. 167: 410–428.
- 453 Elowitz, M. B. et al. 2002. Stochastic gene expression in a single cell. - Science (80-. ). 297: 1183–  
454 1186.
- 455 Endler, J. A. 1986. Natural selection in the wild (RM May, Ed.). - Princeton University Press.
- 456 Evans, S. N. and Steinsaltz, D. 2007. Damage segregation at fissioning may increase growth rates: a  
457 superprocess model. - Theor. Popul. Biol. 71: 473–90.
- 458 Finch, C. and Kirkwood, T. B. 2000. Chance, Development, and Aging. - Oxford University Press.
- 459 Fiske, I. J. et al. 2008. Effects of Sample Size on Estimates of Population Growth Rates Calculated  
460 with Matrix Models (M Rees, Ed.). - PLoS One 3: e3080.
- 461 Fitzpatrick, S. W. et al. 2016. Gene flow from an adaptively divergent source causes rescue through  
462 genetic and demographic factors in two wild populations of Trinidadian guppies. - Evol. Appl. 9:  
463 879–891.
- 464 Gangan, M. S. and Athale, C. A. 2017. Threshold effect of growth rate on population variability of  
465 *Escherichia coli* cell lengths. - R. Soc. open Sci. 4: 160417.
- 466 Gómez, J. M. G. 2010. Aging in bacteria, immortality or not—a critical review. - Curr. Aging Sci. 3:  
467 198–218.
- 468 Hamilton, W. D. 1966. The moulding of senescence by natural selection. - J. Theor. Biol. 12: 12–45.
- 469 Hartemink, N. et al. 2017. Stochasticity, heterogeneity, and variance in longevity in human  
470 populations. - Theor. Popul. Biol. 114: 107–116.
- 471 Hartl, D. J. and Clark, A. G. 2007. Principles of population genetics. - Sinauer.

- 472 Helmstetter, C. E. 1968. DNA synthesis during the division cycle of rapidly growing *Escherichia coli*  
473 B/r. - *J. Mol. Biol.* 31: 507–18.
- 474 Hubbell, S. P. 2001. The unified neutral theory of biodiversity and biogeography (SA Levin and HS  
475 Horn, Eds.). - Princeton University Press.
- 476 Johnson, L. R. and Mangel, M. 2006. Life histories and the evolution of aging in bacteria and other  
477 single-celled organisms. - *Mech. Ageing Dev.* 127: 786–93.
- 478 Jones, O. R. et al. 2014. Diversity of ageing across the tree of life. - *Nature* in press.
- 479 Kennedy, B. K. 1994. Daughter cells of *Saccharomyces cerevisiae* from old mothers display a reduced  
480 life span. - *J. Cell Biol.* 127: 1985–1993.
- 481 Kirkwood, T. B. L. et al. 2005. What accounts for the wide variation in life span of genetically identical  
482 organisms reared in a constant environment? - *Mech. Ageing Dev.* 126: 439–443.
- 483 Lande, R. et al. 2003. Stochastic population dynamics in ecology and conservation.
- 484 Leigh, E. G. 2007. Neutral theory: a historical perspective. - *J. Evol. Biol.* 20: 2075–91.
- 485 Lindner, A. B. and Demarez, A. 2009. Protein aggregation as a paradigm of aging. - *Biochim. Biophys.*  
486 *Acta* 1790: 980–96.
- 487 Lindner, A. B. et al. 2008. Asymmetric segregation of protein aggregates is associated with cellular  
488 aging and rejuvenation. - *Proc. Natl. Acad. Sci. U. S. A.* 105: 3076–81.
- 489 López-Otín, C. et al. 2013. The hallmarks of aging. - *Cell* 153: 1194–217.
- 490 Medawar, P. B. 1952. An unsolved problem of biology. - In: *Uniqueness of the Individual*. H. K.  
491 Lewis, in press.
- 492 Metcalf, C. J. E. 2016. Invisible Trade-offs: Van Noordwijk and de Jong and Life-History Evolution. -  
493 *Am. Nat.* 187: iii–v.
- 494 Nyström, T. et al. 2007. A Bacterial Kind of Aging. - *PLoS Genet.* 3: e224.
- 495 Raj, A. and van Oudenaarden, A. 2008. Nature, nurture, or chance: stochastic gene expression and its  
496 consequences. - *Cell* 135: 216–26.
- 497 Reshes, G. et al. 2008. Timing the start of division in *E. coli*: a single-cell study. - *Phys. Biol.* 5:  
498 46001.
- 499 Roach, D. A. 2012. Age, growth and size interact with stress to determine life span and mortality. -  
500 *Exp. Gerontol.* 47: 782–6.
- 501 Schiemer, F. 1982. Food Dependence and Energetics of Freelifing Nematodes. II. Life History  
502 Parameters of *Caenorhabditis briggsae* (Nematoda) at Different Levels of Food Supply. -  
503 *Oecologia* 54: 122–128.



- 504 Stearns, S. C. 1992. The evolution of life histories. - Oxford University Press Oxford.
- 505 Steiner, U. K. and Tuljapurkar, S. 2012. Neutral theory for life histories and individual variability in  
506 fitness components. - Proc. Natl. Acad. Sci. U. S. A. 109: 4684–9.
- 507 Steiner, U. K. et al. 2010. Dynamic heterogeneity and life history variability in the kittiwake. - J. Anim.  
508 Ecol. 79: 436–44.
- 509 Steiner, U. K. et al. 2012. Trading stages: life expectancies in structured populations. - Exp. Gerontol.  
510 47: 773–81.
- 511 Steiner, U. K. et al. 2014. Generation time, net reproductive rate, and growth in stage-age-structured  
512 populations. - Am. Nat. 183: 771–83.
- 513 Steiner, U. K. et al. 2017. Two stochastic processes shape diverse senescence patterns in a single-cell  
514 organism. - bioRxiv doi.org/10.1101/105387.
- 515 Stewart, E. J. et al. 2005. Aging and death in an organism that reproduces by morphologically  
516 symmetric division. - PLoS Biol. 3: e45.
- 517 Travis, J. et al. 2014. Chapter One – Do Eco-Evo Feedbacks Help Us Understand Nature? Answers  
518 From Studies of the Trinidadian Guppy. - In: Advances in Ecological Research. pp. 1–40.
- 519 Tuljapurkar, S. et al. 2009. Dynamic heterogeneity in life histories. - Ecol. Lett. 12: 93–106.
- 520 Tyedmers, J. et al. 2010. Cellular strategies for controlling protein aggregation. - Nat. Rev. Mol. cell  
521 Biol. 11: 777–788.
- 522 van Noordwijk, A. J. and de Jong, G. 1986. Acquisition and Allocation of Resources: Their Influence  
523 on Variation in Life History Tactics. - Am. Nat. 128: 137.
- 524 Vindenes, Y. and Langangen, Ø. 2015. Individual heterogeneity in life histories and eco-evolutionary  
525 dynamics (J-M Gaillard, Ed.). - Ecol. Lett. 18: 417–432.
- 526 Wang, P. et al. 2010. Robust growth of Escherichia coli. - Curr. Biol. 20: 1099–103.
- 527 Williams, G. C. 1957. Pleiotropy, Natural Selection, and the Evolution of Senescence. - Evolution (N.  
528 Y). 11: 398.
- 529
- 530

Table 1: Notation and Equations

Description	Equation	Notes
	$e_t$	Vector of zeros with a 1 at position $t$ (here $t=1$ for all estimations because of the Leslie matrix structure)
	$e^T$	Vector of ones, superscript $T$ denote transpose
Identity matrix	<b>I</b>	
Population projection matrix (here Leslie matrix)	<b>A</b>	with <b>A</b> = ( <b>F</b> + <b>P</b> )
Stage transition matrix	<b>P</b>	Includes survival rates as off diagonal parameters for non-zero matrix elements
Fertility matrix	<b>F</b>	Includes division rates as first row parameters for non-zero matrix elements.
Population growth rate	$\lambda$ =dominant Eigenvalue of <b>A</b>	
Right eigenvector corresponding to dominant eigenvalue of <b>A</b>	$\omega$ , normalized so to sum of components=1	
Left eigenvector corresponding to dominant eigenvalue of <b>A</b>	$v$ , normalized so to $v_1 = 1$	
Generation time	$T = (\lambda * v * \omega)/(v * \mathbf{F} * \omega)$	
Stage duration matrix	<b>N</b> = ( <b>I</b> - <b>P</b> ) <sup>-1</sup>	Elements quantify the expected time spent in each age conditional on the birth stage (here all individuals are born to stage 1= age 1)
Mean Lifespan strain $i$	$exL_i = e^T * \mathbf{N} * e_t$	

$$exLsq_i = e^T * (2\mathbf{N} - \mathbf{I}) * \mathbf{N} * e_t$$

Variance in lifespan  
strain  $i$

$$VarL_i = exLsq_i - (exL_i)^2$$

$$\hat{\mathbf{F}} = \text{diag}(\mathbf{F})$$

Diagonal elements of fertility  
matrix (here first row fertility  
values)

Expected reproduction  
strain  $i$

$$exR_i = e_t^T * \mathbf{F} * \mathbf{N} * e_t$$

$$exRsq_i = e_t^T * \mathbf{F} * (2\mathbf{N} - \mathbf{I}) * \hat{\mathbf{F}} * \mathbf{N} * e_t$$

Variance in reproduction  
strain  $i$

$$VarexR_i = exRsq_i - (exR_i)^2$$

Cohort generation matrix

$$\mathbf{A}_c = \mathbf{F} * \mathbf{N}$$

Right eigenvector  
corresponding to  
dominant eigenvalue of  
 $\mathbf{A}_c$

$c\omega$ , normalized so to sum of components=1

Left eigenvector  
corresponding to  
dominant eigenvalue of  
 $\mathbf{A}_c$

$cv$ , normalized so to  $(cv^T * c\omega) = 1$

Cohort generation time

$$T_c = (cv^T * \mathbf{N} * c\omega) / (cv^T * c\omega)$$


---

Details and proofs of equations are found elsewhere (Steiner et al. 2012, 2014)

531

532

533

Table 2: Key demographic parameters of the seven isogenic strains

Strain	$\lambda$	T	$T_c$	Mean Lifespan	SD Lifesp.	CV Lifesp.	Mean LRS ( $R_0$ )	SD LRS ( $R_0$ )	CV LRS ( $R_0$ )	# Individuals
AB1157	2.02	2.50	31	23	28	1.2	42	54	1.3	504
BW25113	2.25	2.34	77	54	24	0.4	128	57	0.4	482
IAI1	1.74	3.29	69	44	31	0.7	74	56	0.8	312
MG1655 Inlag	2.24	2.36	43	34	26	0.8	72	57	0.8	519
MG1655 LM	2.18	2.30	44	34	26	0.8	67	54	0.8	505
W3110	2.03	2.38	38	27	27	1.0	50	54	1.1	501
MG1655	1.97	2.83	68	46	31	0.7	94	65	0.7	1017
										<b>3840</b>

534